A Relative Rotation between Two Overlapping UAV's Images

Martinus Edwin Tjahjadi
Department of Geomatics
National Institute of Technology
(ITN) Malang
Malang, Indonesia
edwin@lecturer.itn.ac.id

Fransisca Dwi Agustina
Department of Geomatics
National Institute of Technology
(ITN) Malang
Malang, Indonesia
siscaagustina02@gmail.com

***Abstract*— In this paper, we study the influence of varying baseline components on the accuracy of a relative rotation between two overlapping aerial images taken form unmanned aerial vehicle (UAV) flight. The case is relevant when mosaicking UAV's aerial images by registering each individual image. Geotagged images facilitated by a navigational grade GPS receiver on board inform the camera position when taking pictures. However, these low accuracies of geographical coordinates encoded in an EXIF format are unreliable to depict baseline vector components between subsequent overlapping images. This research investigates these influences on the stability of rotation elements when the vector components are entered into a standard coplanarity condition equation to determine the relative rotation of the stereo images. Assuming a nadir looking camera on board while the UAV platform is flying at a constant height, the resulted vector directions are utilized to constraint the coplanarity equation. A detailed analysis of each variation is given. Our experiments based on real datasets confirm that the relative rotation between two successive overlapping images is practically unaffected by the accuracy of positioning method. Furthermore, the coplanarity constraint is invariant with respect to a translation along the baseline of the aerial stereo images.**

Keywords*— *UAV, Relative, Pose, Orientation, Stereoscopic Processing

I. INTRODUCTION

In supporting a large scale urban city mapping [1] from UAV's images, mosaicking and compositing aerial images [2], as well as stereo matching [3], it is necessary to determine a three-dimensional motion of a rigid object (i.e. a flying UAV platform) from perspective images. A relative orientation process recreates relative translation and angular relationships between two successive overlapping images that existed at the time of photography. A relative orientation consisting of translation and rotation in the stereo images is a prerequisite to retrieve 3D structures from images. The most fundamental problem in geometric computer vision and photogrammetry is a determination of the relative orientation or relative pose from point correspondences between two images.

Numerous works for recovering the position and orientation of stereo images have been shown. Early attempts to reconstruct a scene from the position and rotation from image correspondences utilize projective theory on a coplanarity constraint [4-7]. A solid theoretical foundation about projective significance of the relative orientation matrix was recognized, which is known as the Fundamental/Essential matrix for describing the geometry of an image pair. Algebraic projective geometry is used to generate polynomial system iteratively to yield an optimal and exact Essential matrix. This method uses 8 point correspondences to the approximate values, then enters into the least squares adjustment with linearized version of the system. One major drawback is the low stability of the system and its use of Gauss-Newton elimination being susceptible to all types of perturbations [8].

Seminal achievements of the scene reconstruction based on this matrix are due to Longuet-Higgins [9] together with Tsai and Huang [10]. They pioneer a further work on the relative orientation improvements. Different strategies and different numbers of minimal correspondences are used to solve the intractable problem using this simplest matrix. For examples, the use of orthogonalization algorithm [11], eigenvectors and eigenvalues [12], singular value decomposition (SVD) [10], quaternions [13], and normalized image coordinates [14] increases the stability and reliability of the resulting matrix. Although an existence of the Essential matrix can be determined with a minimum number of four or fewer point correspondences [15], the most stable and linearly unique solution is given by [14] which use eight point correspondences or more. Other methods using five to seven point correspondences are outlined in [16-18].

Other methods of determining the relative orientation are by exploiting coplanarity condition of the two adjacent images as shown in Fig.1. The geometry of the point correspondence reveals the geometric relations between the scene point and the image points. Assuming the scene point P is static and two images are taken from two different places with a calibrated camera, the relative orientation is described by the two independent sets of exterior orientation parameters (e.g. 6 parameters of each image and thus 12 parameters altogether). Since the scene point object will be reconstructed up to a spatial similarity transformation, which is comprised of seven parameters (i.e. three translations, three rotations, and one arbitrary scale), it means that only 5 parameters out of the 12 total exterior orientation parameters are determinable. This situation is realized by fixing one image (i.e. left image) such that the pose of these images is relatively oriented with respect to each other. Hence, the object points can be reconstructed at an arbitrary scale only up to spatial similarity transformation, or so called a photogrammetric model. Thus, the rotation matrix $\boldsymbol{R}_2$ of the right image and the direction of the baseline $\boldsymbol{b}$ connecting two projection center O_1 and O_2 are chosen as the parameters of the relative orientation.

XXX-X-XXXX-XXXX-X/XX/$XX.00 ©20XX IEEE
978-1-5386-8402-3/18/$31.00 ©2018 IEEE

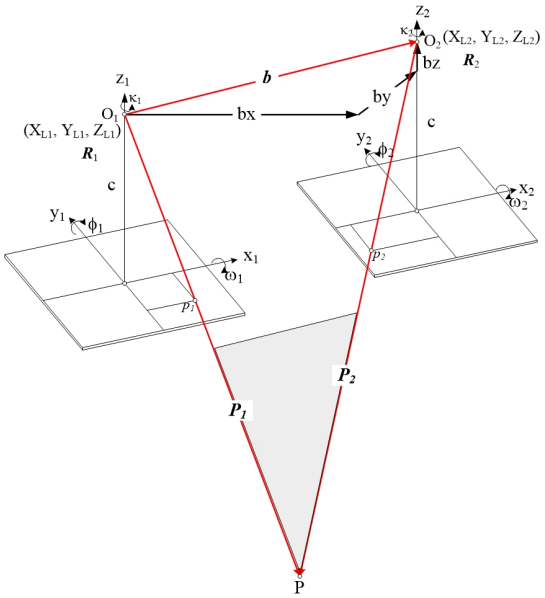

Fig. 1. Relative orientation with a fixed left image

A direct method to determine these parameters based on the coplanarity constraint is reported in [19-24]. It is derived by direct linear transformation (i.e. DLT) from coplanarity condition equation and this method is linear with respect to the 8 unknown parameters [21, 22]. A direct solution for these parameters can be achieved without knowing any approximate values. However, a duality problem of a solution is still exhibited [22]. Attempts to improve the solution are also reported. An alternative approach by imposing four non-linear constraints by deriving inherent orthogonal properties of rotation matrix [20] improves the solution. Another attempt is by adding seven constraints to control and adjust the solution parameters [19]. Six constraints are deduced from the orthogonality of the rotation matrix, and the last one arises from the decomposition of baseline. Furthermore, an attempt to incorporate a RANSAC algorithm in the method to filter out gross errors in the relative orientation solution is also reported by [24].

Instead of decomposing the essential matrix into the rotation and translation parameters of the pose in the direct method, the rotational and translation elements are directly computed into the coplanarity condition. If the epipolar plane defined by the vector of $\boldsymbol{b}$, $\boldsymbol{P}_1$ and $\boldsymbol{P}_2$, which also contain the image point p_1 and p_2, the computational solution of relative orientation utilizes the condition that an object point P and the two perspective centers of O_1 and O_2 must lie in a plane (coplanarity constraint). The coplanarity equation is a scalar triple product of a volume of a parallelepiped of these three vectors. If the base of the parallelepiped defined by the any first two out of three vectors and its height by the remaining one, the volume of parallelepiped will be zero if the third vector lies in the plane of the base, making it coplanar with the first two vectors. Direct linear solution of this method uses an extensive algebraic manipulation [21, 22], however a duality of the solution arise due to perturbations in image point coordinates. To remedy the result, further constraints are applied to eliminate the influence of over parameterization of the direct relative orientation model [19, 20, 24]. These improved methods are claimed to be more suitable for UAV flying at low altitudes.

Recent advances in a UAV's low cost direct geo-referencing utilizing a navigational grade of a GPS/GNSS board mounted on the aerial platform [25] provides additional 3D information about geographical coordinates encoded in an EXIF format [26] on each captured images. This low level accuracy of coordinates in geotagged images gives a baseline vector $\boldsymbol{b}$ between two successive overlapping images. Since the 3D coordinates of each image are known, therefore the 3D baseline vector between each projection center of each image can be determined. Hence a further constraint on the coplanarity condition can be imposed by these baseline vectors. This paper, therefore, investigates a feasibility of utilizing this vector to determine the relative rotation between two overlapping images. Algebraic manipulations will be elaborated to justify the method in the following sections.

II. Research Metodology

The coplanarity condition in Fig. 1 implies a situation in which the object point P and its corresponding image point p_1 and p_2 on two overlapping images are located on the same plane with the baseline vector $\boldsymbol{b}$. When this condition is achieved, the vector $\boldsymbol{P}_1$ will have an intersection with the vector $\boldsymbol{P}_2$, and these vectors together with the baseline vector $\boldsymbol{b}$ will be coplanar and the scalar triple product of them is zero. The mathematical model in a determinant form of one pair of corresponding point is given by:

$$\boldsymbol{F} = \boldsymbol{b}.(\boldsymbol{P}_1 \times \boldsymbol{P}_2) = \begin{vmatrix} b_x & b_y & b_z \\ U_1 & V_1 & W_1 \\ U_2 & V_2 & W_2 \end{vmatrix} = 0 \qquad (1)$$

$$\boldsymbol{b} = \begin{bmatrix} b_x \\ b_y \\ b_z \end{bmatrix} = [X_{L2} - X_{L1} \quad Y_{L2} - Y_{L1} \quad Z_{L2} - Z_{L1}]^T \qquad (2)$$

$$\boldsymbol{P}_1 = [U_1 \quad V_1 \quad W_1]^T = \boldsymbol{R}_1^T [x_1 \quad y_1 \quad -c]^T \qquad (3)$$

$$\boldsymbol{P}_2 = [U_2 \quad V_2 \quad W_2]^T = \boldsymbol{R}_2^T [x_2 \quad y_2 \quad -c]^T \qquad (4)$$

Equation (1) is the coplanarity condition in the form of a scalar triple product of the volume of a parallelepiped. Its determinant form consists of three vector components of $\boldsymbol{b}$, $\boldsymbol{P}_1$ and $\boldsymbol{P}_2$. A determinable baseline vector of **b** (2) is obtained by extracting geographical coordinates of the two perspective centers of O_1 and O_2 of the left image and the right image respectively. A subtraction of Cartesian coordinates of its geographical ones is sufficient to define the baseline components of the two perspective centers. The Cartesian coordinates are expressed as the X_{L1}, Y_{L1} and Z_{L1} of the perspective center of the left image as well as the X_{L2}, Y_{L2} and Z_{L2} of the perspective center of the right image. The vector $\boldsymbol{P}_1$ in (3) and $\boldsymbol{P}_2$ in (4) represent the object space vector from the image point p_1 and p_2 on the left and the right image respectively. A rotation matrix $\boldsymbol{R}$ rotates object space vectors into vectors in the image or model coordinates system. It is a 3 by 3 matrix whose elements constitute the exterior orientation parameters with rotation angles of ω, ϕ, κ [27]:

$$\boldsymbol{R} = \begin{bmatrix} c\phi c\kappa & c\omega s\kappa + s\omega s\phi c\kappa & s\omega s\kappa - c\omega s\phi c\kappa \\ -c\phi s\kappa & c\omega c\kappa - s\omega s\varphi s\kappa & s\omega c\kappa + c\omega s\phi s\kappa \\ s\phi & -s\omega c\phi & c\omega c\phi \end{bmatrix} \qquad (5)$$

where the cosine and sine of trigonometric functions are abbreviated to 'c' and 's' respectively.

Here it is assumed that two images have an equal focal length c and principal point offsets. Also image coordinate on each image have been corrected for the principal point offset. If the left image is fixed and the origin of the local 3D model is located in the projection center of the left image and oriented parallel to its image coordinate system, the exterior orientation parameters can be chosen as $X_{L1} = Y_{L1} = Z_{L1} = 0$, also $\omega_1 = \phi_1 = \kappa_1 = 0$. Therefore the vector $\boldsymbol{P}_1$ can be reduced to:

$$\boldsymbol{P}_1 = [U_1 \quad V_1 \quad W_1]^T = [\boldsymbol{I}]\ [x_1 \quad y_1 \quad -c]^T \tag{6}$$

Now the right image is oriented in the model coordinate system by 3 translations and 3 rotations: $X_{L2} = b_x$, $Y_{L2} = b_y$, $Z_{L2} = b_{z,}$ and ω_2, ϕ_2, κ_2. The vector of $\boldsymbol{P}_2$ in (4) can be expanded into:

$$\boldsymbol{P}_2 = \begin{bmatrix} c\phi_2 c\kappa_2 & -c\phi_2 s\kappa_2 & s\phi_2 \\ c\omega_2 s\kappa_2 + s\omega_2 s\phi_2 c\kappa_2 & c\omega_2 c\kappa_2 - s\omega_2 s\phi_2 s\kappa_2 & -s\omega_2 c\phi_2 \\ s\omega_2 s\kappa_2 - c\omega_2 s\phi_2 c\kappa_2 & s\omega_2 c\kappa_2 + c\omega_2 s\phi_2 s\kappa_2 & c\omega_2 c\phi_2 \end{bmatrix} \begin{bmatrix} x_2 \\ y_2 \\ -c \end{bmatrix} \tag{7}$$

From (7) it is clear that the elements of $[U_2 \quad V_2 \quad W_2]^T$ are a multiplication of a transposed rotation matrix and a vector of the image coordinates in the right image.

The known baseline vector $\boldsymbol{b}$ is defined by the base components of b_x, b_y and b_z connecting the two perspective center O_1 and O_2. Suppose the perspective center O_2 is displaced along the baseline toward O_1, it is clear from the Fig.1 that the vector $\boldsymbol{P}_2$ will still be coplanar with the baseline $\boldsymbol{b}$ and that the vector will intersect in a point lying on the line between O_1 and p_1. From a relation of similar triangles, the scale of the model will be directly proportional to the length of the baseline. Therefore, the model coordinate system can be scaled by an arbitrary factor depending of the choice of the baseline length. For simplicity, the longest component of the baseline vector is set to a constant value of b'_x (i.e. $b'_x = b_x/b_x = 1$). As a consequence of these facts, the other two baseline components are adjusted accordingly into $b'_y = b_y/b_x$ and $b'_z = b_z/b_x$. These divisions mean that a direction of the unit vector of the baseline components remains constant irrespective of the baseline length chosen. Now, three rotation elements only out of five elements of the relative orientation remained. The computational solution of (1) can be simplified into:

$$\boldsymbol{F} = \boldsymbol{b}.(\boldsymbol{P}_1 \times \boldsymbol{P_2}) = \begin{vmatrix} 1 & b'_y & b'_z \\ x_1 & y_1 & -c \\ U_2 & V_2 & W_2 \end{vmatrix} = 0 \tag{8}$$

The coplanarity condition of (8) is only fulfilled if vector $\boldsymbol{P}_1$ and $\boldsymbol{P}_2$ intersect in object point P if the position of image point p_1 and p_2, as well as the orientation parameter of the right image are assumed to be an error free. For each pair of correspondent points one coplanarity equation can be derived. The calculation of the three rotational elements of the relative orientation follows the principle least squares adjustment. The observed quantities are the image coordinates refined for the any systematic error. A general form here,

$$ {}_r\boldsymbol{F}_1^0 + {}_r\boldsymbol{A}_n\ {}_n\boldsymbol{v}_1 + {}_r\boldsymbol{B}_u\ {}_u\Delta_1 = {}_r\boldsymbol{O}_1 \tag{9}$$

while $\boldsymbol{F}$ is evaluated at the approximate value of (8), $\boldsymbol{A}$ is a row matrix which consists of the partial derivatives of $\boldsymbol{F}$ with respect to each of the observed quantities, $\boldsymbol{v}$ is composed of the residuals to the observation, $\boldsymbol{B}$ is a row matrix composed of the partial derivatives of $\boldsymbol{F}$ with respect to the rotational elements of parameters, Δ is column vector composed of the alteration to the approximate values of the parameters. The subscript n shows the number of observed values of observable quantities, the subscript u shows the number of unknown quantities (i.e. 3 rotational parameters), and the subscript r indicates the number of condition equations where both observed and unknown quantities are present or it equals to the number of correspondences. Since there are four image coordinate measurements for each corresponding point, here n = 4r. The matrices of each point of observation will be as follows,

$$\boldsymbol{A}_i = [\partial F_i/\partial x_{1i} \quad \partial F_i/\partial y_{1i} \quad \partial F_i/\partial x_{2i} \quad \partial F_i/\partial y_{2i}] \tag{10}$$

$$\boldsymbol{B}_i = [\partial F_i/\partial \omega_2 \quad \partial F_i/\partial \phi_2 \quad \partial F_i/\partial \kappa_2] \tag{11}$$

$$\boldsymbol{v}_i = [v_{x_{1i}} \quad v_{y_{1i}} \quad v_{x_{2i}} \quad v_{y_{2i}}]^T \tag{12}$$

$$\Delta = [\delta\omega_2 \quad \delta\phi_2 \quad \delta\kappa_2]^T \tag{13}$$

where the subscript of i shows the index of the i^{th} correspondence point. Therefore for the number of r correspondence points, the full matrices would be as follows

$${}_r\boldsymbol{A}_n = \begin{bmatrix} \boldsymbol{A}_1 & 0 & 0 & \cdots & 0 \\ 0 & \boldsymbol{A}_2 & 0 & \cdots & 0 \\ 0 & 0 & \boldsymbol{A}_3 & \cdots & 0 \\ \vdots & \vdots & \vdots & \ddots & \vdots \\ 0 & 0 & 0 & \cdots & \boldsymbol{A}_r \end{bmatrix};\ {}_r\boldsymbol{B}_u = \begin{bmatrix} \boldsymbol{B}_1 \\ \boldsymbol{B}_2 \\ \boldsymbol{B}_3 \\ \vdots \\ \boldsymbol{B}_r \end{bmatrix} \tag{14}$$

$${}_r\boldsymbol{F}_1^0 = \begin{bmatrix} \boldsymbol{F}_1^0 \\ \boldsymbol{F}_2^0 \\ \vdots \\ \boldsymbol{F}_r^0 \end{bmatrix};\ {}_u\Delta_1 = \begin{bmatrix} \delta\omega \\ \delta\phi \\ \delta\kappa \end{bmatrix};\ {}_{4r}\boldsymbol{v}_1 = \begin{bmatrix} \boldsymbol{v}_1 \\ \boldsymbol{v}_2 \\ \vdots \\ \boldsymbol{v}_r \end{bmatrix} \tag{15}$$

In the case of approximately parallel nadir viewing directions, the initial values for linearization of the rotation parameters can be set to zero. The $\boldsymbol{F}^0$ is the volume of parallelepiped calculated from the initial values. The approximate values are iteratively improved by the adjusted correction until there is no significant change. The difference coefficient as well as their partial derivatives can be computed using determinants as follows,

$$\partial F/\partial x_1 = \left(b'_z V_2 - b'_y W_2\right) \tag{16}$$

$$\partial F/\partial y_1 = (W_2 - b'_z U_2) \tag{17}$$

$$\frac{\partial F}{\partial x_2} = \begin{vmatrix} 1 & b'_y & b'_z \\ x_1 & y_1 & -c \\ r_{11} & r_{12} & r_{13} \end{vmatrix};\ \frac{\partial F}{\partial y_2} = \begin{vmatrix} 1 & b'_y & b'_z \\ x_1 & y_1 & -c \\ r_{21} & r_{22} & r_{23} \end{vmatrix} \tag{18}$$

$$\frac{\partial F}{\partial \omega_2} = \begin{vmatrix} 1 & b'_y & b'_z \\ x_1 & y_1 & -c \\ 0 & -W_2 & V_2 \end{vmatrix} \tag{19}$$

$$\frac{\partial F}{\partial \phi_2} = \begin{vmatrix} 1 & b'_y & b'_z \\ x_1 & y_1 & -c \\ -V_2\, s\omega + W_2\, c\omega & U_2\, s\omega & -U_2\, c\omega \end{vmatrix} \quad (20)$$

$$\frac{\partial F}{\partial \kappa_2} = \begin{vmatrix} 1 & b'_y & b'_z \\ x_1 & y_1 & -c \\ x_2 r_{21} - y_2 r_{11} & x_2 r_{22} - y_2 r_{12} & x_2 r_{23} - y_2 r_{13} \end{vmatrix} \quad (21)$$

Equations (16) to (21) are partial derivatives with respect to the measurable quantities and unknown parameters. Partial derivatives with respect to the observation of coordinates of the left image are (16) and (17), and of the right image is (18) respectively. Also, partial derivatives of the unknown rotational parameters are expressed in (19) to (21).

III. Results and Analysis

Field observations were carried out in Malang city. An array of 30 ground control points (GCPs) is established from a white concentric ring surrounded with dark background for point correspondences (Fig.2). To avoid false matches and to facilitate a possible highest accuracy of image coordinate measurements of GCPs on stereo images, least squares image matching are performed [3] to seek the best matches on stereo images as illustrated in Fig. 3. Furthermore, the matched points of the stereo images are represented in Table 1. The images are calibrated with a fixed focal length of 35mm and the image coordinates are corrected for the principal point offset. Table 1 shows image coordinates of the left and right image in a metric unit instead of pixels.

Fig. 2. GCPs on the Field

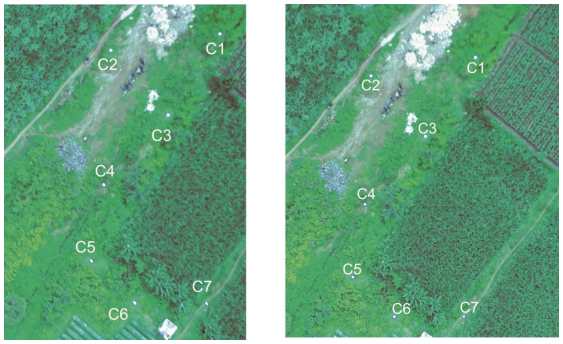

Fig. 3. Some of the correspondence points from cropped stereo images

TABLE I. Correspondence Points Coordinates

Point	Left Image		Right Image	
	x (mm)	*y (mm)*	*x (mm)*	*y (mm)*
C1	14.0175	6.5637	7.2925	7.9013
C2	9.9706	5.9494	3.1806	7.1694
C3	12.1038	3.5562	5.3250	4.7850
C4	9.7106	0.9813	2.9463	2.1119
C5	9.2606	-1.8444	2.4706	-0.7519
C6	10.8625	-3.4025	4.1013	-2.3125
C19	3.0850	-0.2513	-3.7700	0.7838
C20	4.7381	0.4644	-2.1375	1.5269
C21	0.2063	3.9688	-6.6509	4.9800
C22	-1.5253	5.4694	-8.3613	6.4506

From the geotagged left image and right image (Fig.3), geographical coordinates are readily available in an EXIF format on each image and they are used to determine projective center coordinates. The result of the projective coordinates of each image is shown in Table 2. It shows a converted Cartesian coordinates from the geographical coordinates. The conversion is performed using widely available open source software.

TABLE II. Cartesian Coordinates in WGS-84

	Projective Center of Geotagged Images	
	Left Image	*Right Image*
X_L (m)	674879.6511	674873.7796
Y_L (m)	9121309.6780	9121357.8162
Z_L (m)	809.1911	807.6767

The projective center coordinates of each image in the Cartesian coordinate system are then utilized to calculate the baseline vector components between two images as in (2). If the GCPs are surveyed using geodetic type of GPS, the obtained geographical coordinates can be verified using space resection methods [27-29]. The resection method needs at least three GCPs appeared on both images. The baseline vector is shown in the second column of Table 3. The third column is occupied by the Unit Vector. The unit vector of the baseline is calculated by dividing each component by the length of the baseline ***b***. Also, the normalized unit vector in the last column is obtained by dividing each unit vector component by the largest element, in this case is b_x. A result of these calculations is presented in Table 3.

TABLE III. Baseline Vector, Unit Vector, and Normalized Unit Vector

	Baseline Components		
	Vector (m)	*Unit Vector*	*Normalized Unit Vector*
b_x	48.1382	0.992159777	1
b_y	-5.8715	-0.12101545	-0.12197174
b_z	-1.5144	-0.03121277	-0.031459423

A reason to categorize the components into three types shown in Table 3 is to ascertain the influence of the baseline length to the accuracy and stability of rotational parameters of the relative orientation. Due to inaccuracies of the geographical coordinates from the GPS that might influence the resulted rotational parameters, it is a logical decision to decouple its vector components into its unit vectors for maintaining common directions of the baseline vector. To compute the parameters, the vector and the unit vector components in the Table 3 are enter into (1), meanwhile the normalized unit vector components are entered into (8). Iterative least squares adjustments of (9) are used to obtain a solution of (13). Results of the rotational parameters in terms of Euler angles parameterizations are presented in Table 4.

TABLE IV. ROTATION PARAMETERS

	Rotation Elements (degrees)		
	Vector	***Unit Vector***	***Normalized Unit Vector***
ω_2	-0.71645164	-0.71645164	-0.71645164
ϕ_2	2.75634010	2.75634010	2.75634010
κ_2	-0.65907221	-0.65907221	-0.65907221

Table 4 shows the rotation parameters are remain stable irrespective of the baseline types chosen. It reveals that the rotation parameters are invariant under a change of baseline length as long as its direction of the unit vector remains constant. In other words, imprecisions of the geotagged coordinates in determining the baseline vectors between two images have little or no influence on the numerical stability of the rotation parameters. Evidence shows that all root mean square errors of the projection error on the left image and on the right image for all types are relatively stable of around 0.00171 mm and 0.00168 mm respectively. For example, the projection errors of the type of "unit vector" baseline on both images are illustrated on Table 5.

TABLE V. TYPICAL PROJECTION ERRORS ON TYPE OF "UNIT VECTOR" ON STEREO IMAGES

Point	**Projection Error**			
	Left Image ($x10^{-3}$mm)		***Right Image ($x10^{-3}$mm)***	
	x	***y***	***x***	***y***
C1	0.1719	1.9986	-0.1233	-1.9490
C2	-0.2971	-3.5082	0.2179	3.4425
C3	0.1526	1.8684	-0.1159	-1.8311
C4	-0.1979	-2.5404	0.1584	2.5028
C5	-0.0026	-0.0351	0.0022	0.0347
C6	0.0823	1.1424	-0.0714	-1.1272
C19	-0.0177	-0.2348	0.0148	0.2337
C20	-0.0243	-0.3163	0.0199	0.3140
C21	0.0762	0.9412	-0.0594	-0.9378
C22	0.0546	0.6594	-0.0416	-0.6579

Based on the small number of projection error presented in the Table 5, it indicates that inaccuracies of the GPS coordinates from the navigational solutions have little or no influence on the rotation parameter results. No matter what the base line is expressed as a vector, unit vector, or a normalized unit vector, the rotational element results remain stable. For comparison purpose, a classical photogrammetric relative orientation is computed using the same image coordinates as shown in the Table 1. As a rule of thumb, the b_x component is usually set to 1, and the result of five other parameters is presented in the Table 6.

TABLE VI. PHOTOGRAMMETRIC RELATIVE ORIENTATIONPARAMETERS

Parameter	**Relative Orientation Value**
b_y	-0.075552
b_z	-0.047
ω_2(degree)	-0.7164264
ϕ_2(degree)	2.7563281
κ_2(degree)	-0.6590734

Table 6 shows the result of all parameters of photogrammetric relative orientation. As expected, the base line components of b_y and b_z are different from that of the baseline components presented in Table 3, since both are free or unconstraint parameters in a classical relative orientation. On the other hand, all the rotational parameters have very slight differences from that of presented in the Table 4. These very tiny deviations are reasonable since a slight change of the baseline components can change the baseline's direction, and as a result it can also change rotational parameters. Overall, by comparing Table 4 and Table 6, the rotational parameters of the relative orientation are unaffected by a changing of baseline vector components as long as its vector direction is unchanged.

IV. CONCLUSION

The most important achievement of this paper is to demonstrate that the rotation parameters of the relative orientation are invariant with respect to the translation along the image projection centers. The relative rotation between two successive overlapping images is practically unaffected by the accuracy of positioning method. Whilst geotagged images are readily available, their coordinates can be utilized to constraint the classical relative orientation computational procedures, hence fewer point correspondences are needed to compute the relative orientation parameters. Constraining baseline parameters of the relative orientation by the navigational grades of GPS coordinates can speed up the computational process and this procedure can readily be integrated into a RANSAC algorithm to produce a faster and more stable direct close form solution of relative orientation.

ACKNOWLEDGMENT

The author wishes to express his sincere thanks to Ministry of Research, Technology and Higher Education of the Republic of Indonesia for supporting a research grant "Penelitian Terapan Unggulan Perguruan Tinggi (PTUPT)", with a contract number of 120/SP2H/LT/DRPM/2018 and ITN.03.0742/IX.REK/2018.

REFERENCES

[1] M. Saadatseresht, A. H. Hashempour, and M. Hasanlou, "UAV Photogrametry: a Practical Solution for Challenging Mapping

Projects," The International Archives of the Photogrammetry, Remote Sensing and Spatial Information Sciences, vol. 40(1/W5), pp. 619-623, November 2015.

[2] M. E. Tjahjadi, F. Handoko, and S. S. Sai, "Novel Image Mosaicking of UAV's Imagery Using Collinearity Condition," International Journal of Electrical and Computer Engineering (IJECE), vol. 7(3), pp. 1188-1196, June 2017.

[3] M. E. Tjahjadi and F. Handoko, "Precise wide baseline stereo image matching for compact digital cameras," in 2017 4th International Conference on Electrical Engineering, Computer Science and Informatics (EECSI), Yogyakarta, Indonesia, pp. 181-186, 2017.

[4] C. M. A. V. D. Hout and P. Stefanovic, "Efficient Analytical Relative Orientation," The ITC Journal, pp. 304-323, 1976.

[5] P. Stefanovic, "Relative Orientation - a New Approach," The ITC Journal, pp. 417-448, 1973.

[6] E. H. Thompson, "A Rational Algebraic Formulation Of The Problem Of Relative Orientation," Photogrammetric Record, vol. 3, pp. 152-159, 1959.

[7] E. H. Thompson, "The Projective Theory of Relative Orientation," Photogrammetria, vol. 23, pp. 67-75, 1968.

[8] U. Helmke, K. Hüper, L. Pei Yean, and J. Moore, "Essential Matrix Estimation Using Gauss-Newton Iterations on a Manifold," International Journal of Computer Vision, vol. 74(2), pp. 117-136, 2007.

[9] H. C. Longuet-Higgins, "A Computer Algorithm for Reconstructing a Scene from Two Projections," Nature, vol. 293(5828), p. 133, 1981.

[10] R. Y. Tsai and T. S. Huang, "Uniqueness and Estimation of Three-Dimensional Motion Parameters of Rigid Objects with Curved Surfaces," IEEE Transactions on Pattern Analysis and Machine Intelligence, vol. 6(1), pp. 13-27, 1984.

[11] J. Weng, T. S. Huang, and N. Ahuja, "Motion and Structure from Two Perspective Views: Algorithms, Error Analysis, and Error Estimation," IEEE Transactions on Pattern Analysis and Machine Intelligence, vol. 11(5), pp. 451-476, 1989.

[12] S. J. Maybank, "Properties of Essential Matrices," International Journal of Imaging Systems & Technology, vol. 2(4), pp. 380-384, September 1990.

[13] B. K. Horn, "Relative Orientation," International Journal of Computer Vision, vol. 4(1), pp. 59-78, 1990.

[14] R. I. Hartley, "In Defense of the Eight-Point Algorithm," IEEE Transactions on Pattern Analysis and Machine Intelligence, vol. 19(6), pp. 580-593, 1997.

[15] S. Agarwal, H.-L. Lee, B. Sturmfels, and R. Thomas, "On the Existence of Epipolar Matrices," International Journal of Computer Vision, vol. 121(3), pp. 403-415, 2017.

[16] D. Nistér, "An Efficient Solution to the Five-Point Relative Pose Problem," IEEE Transactions on Pattern Analysis and Machine Intelligence, vol. 26(6), pp. 756-770, 2004.

[17] H. Stewénius, D. Nistér, F. Kahl, and F. Schaffalitzky, "A minimal solution for relative pose with unknown focal length," Image & Vision Computing, vol. 26(7), pp. 871-877, 2008.

[18] J. Philip, "A Non-Iterative Algorithm for Determining All Essential Matrices Corresponding to Five Point Pairs," Photogrammetric Record, vol. 15(88), pp. 589-599, October, 1996.

[19] Y. Chen, Z. Xie, Z. Qiu, M. Zhang, and S. Zhong, "The model of direct relative orientation with seven constraints for geological landslides measurement and 3D reconstruction," Earth Sciences Research Journal, vol. 20(4), pp. F1-F6, 2016.

[20] Y. Zhang, X. Huang, X. Hu, Fangqi Wan, and L. Lin, "Direct relative orientation with four independent constraints," ISPRS journal of photogrammetry and remote sensing, vol. 66(6), pp. 809-817, 2011.

[21] T. Y. Shih, "RLT: A Closed Form Solution for Relative Orientation," The International Archives of Photogrammetry and Remote Sensing, vol. 30(B5), pp. 357-364, March 1994.

[22] T. Y. Shih, "On the Duality of Relative Orientation," Photogrammetric Engineering And Remote Sensing, vol. 56(9), pp. 1281-1283, 1990.

[23] L. Chao and Z. Yue, "Approach of Camera Relative Pose Estimation Based on Epipolar Geometry," Information Technology Journal, vol. 11(9), pp. 1202-1210, 2012.

[24] J. Wang, Z. Lin, and C. Ren, "Relative Orientation in low Altitude Photogrammetry Survey," The International Archives of the Photogrammetry, Remote Sensing & Spatial Information Sciences, vol. 39(B1), pp. 463-467, 2012.

[25] J. Wang, M. Garratt, A. Lambert, J. J. Wang, S. Han, and D. Sinclair, "Integration of GPS/INS/vision sensors to navigate unmanned aerial vehicles," The International Archives of the Photogrammetry, Remote Sensing and Spatial Information Sciences, vol. 37(B1), pp. 963-970, 2008.

[26] C. F. Lo, M. L. Tsai, K. W. Chiang, C. H. Chu, G. J. Tsai, C. K. Cheng, N. El-Sheimy, and H. Ayman, "The Direct Georeferencing Application and Performance Analysis of UAV Helicopter in GCP-Free Area," The International Archives of the Photogrammetry, Remote Sensing and Spatial Information Sciences, vol. 40(1/W4), pp. 151-157, 2015.

[27] M. E. Tjahjadi and F. Handoko, "Single frame resection of compact digital cameras for UAV imagery," in 2017 4th International Conference on Electrical Engineering, Computer Science and Informatics (EECSI), Yogyakarta, Indonesia, pp. 409-413, 2017.

[28] M. E. Tjahjadi and F. D. Agustina, "Single image orientation of UAV's imagery using orthogonal projection model," in 2017 International Symposium on Geoinformatics (ISyG), Malang, Indonesia, pp. 18-23, 2017.

[29] M. E. Tjahjadi, "A Fast And Stable Orientation Solution of Three Cameras-Based UAV Imageries," ARPN Journal of Engineering and Applied Sciences, vol. 11(5), pp. 3449-3455, 2016.